Production of light nuclei in relativistic heavy-ion collisions

J. Barrette,[3] R. Bellwied,[8] P. Braun-Munzinger,[5] W.E. Cleland,[4] T.M. Cormier,[8] G. David,[5] J. Dee,[5] G.E. Diebold,[9] O. Dietzsch,[7] J.V. Germani,[9] S. Gilbert,[3] S.V. Greene,[9] J.R. Hall,[8] T.K. Hemmick,[5] N. Herrmann,[2] B. Hong,[5] K. Jayananda,[4] D. Kraus,[4] B.S. Kumar,[9] R. Lacasse,[3] D. Lissauer,[1] W.J. Llope,[5] T.W. Ludlam,[1] S. McCorkle,[1] R. Majka,[9] S.K. Mark,[3] J.T. Mitchell,[9] M. Muthuswamy,[5] E. O'Brien,[1] C. Pruneau,[8] F.S. Rotondo,[9] J. Sandweiss,[9] N.C. daSilva,[7] U. Sonnadara,[4] J. Stachel,[5] H. Takai,[1] E.M. Takagui,[7] T.G. Throwe,[1] D. Wolfe,[6] C.L. Woody,[1] N. Xu,[5] Y. Zhang,[5] Z. Zhang,[4] and C. Zou[5]
(The E814 Collaboration)
[1] *Brookhaven National Laboratory, Upton, New York 11973*
[2] *Gesellschaft für Schwerionenforschung, Darmstadt, Germany*
[3] *McGill University, Montreal, Canada H3A 278*
[4] *University of Pittsburgh, Pittsburgh, Pennsylvania 15260*
[5] *Sate University New York, Stony Brook, New York 11794*
[6] *University of New Mexico, Albuquerque, New Mexico 87131*
[7] *University of São Paulo, Brazil*
[8] *Wayne State University, Detroit, MI 48202.*
[9] *Yale University, New Haven, Connecticut 06520*
(Received 2 March 1994)

We have measured cross sections for the synthesis of nuclei of mass A $\leq$ 4 in collisions of 14.6A GeV/c ^{28}Si nuclei with targets of Pb, Cu, and Al. The data are measured at close to center-of-mass rapidities, and are unique in their exploration of the centrality dependence of nucleosynthesis. Simple coalescence models that were used to study nucleosynthesis at lower energies are inadequate for the description of our measurements. Our data and improved models are used to extract parameters related to the size of the interaction volume at freeze-out.

PACS number(s): 25.75.+r

I. INTRODUCTION

Nucleus-nucleus collisions at $\sim$ 15 GeV per nucleon are an effective way to create regions of hot and dense nuclear matter [1]. Several experiments have studied the properties of the collision region through measurements of energy flow, the spectra of particles, and correlations between pairs of emitted particles. In particular, the Hanbury-Brown Twiss technique has been used to study the space-time evolution of the collision volume [2–5]. In this paper we explore an alternative technique to probe this evolution. The abundances of light nuclei created near the center-of-mass velocity (mid rapidity) are expected to probe the latter stages in the evolution of the initially hot, dense nuclear phase. Nucleosynthesis occurs when the collision volume has expanded to low densities, and cooled to sufficiently low temperatures. At this time, nucleons that are still in relatively close physical proximity to one another, and move with small relative momenta, may fuse to form nuclei. The abundances of light nuclei are interesting in their own right, and also enable us to explore the physics of composite particle production. A knowledge of the nuclear production ratios helps us to estimate the probability with which more exotic entities such as antinuclei, multistrange hypernuclei [6], and strangelets [7] may be produced as remnants of the unusual states of matter created in high energy nucleus-nucleus collisions. The relative abundances of light nuclei can also be used to obtain information about entropy production in heavy ion collisions [8].

At lower beam energies, several models have been used to describe the production of light nuclear clusters [9]. Schematically, they relate the production cross section of a cluster of A nucleons to the Ath power of the probability to find a nucleon within a certain volume in momentum space [10]. This power law for light nucleus production was studied extensively at Bevalac energies (few GeV per nucleon) and was used in the description of the trends seen in the data [11]. In this paper we will describe our measurements of the yields of clusters up to A=4 produced in collisions of 14.6A GeV/c ^{28}Si nuclei with Pb, Cu, and Al targets. The measurements cover a range of rapidity (y) between 1.2 and 2.1, near zero transverse momentum (p_t). They are unique in their exploration of the centrality dependence of nucleosynthesis. While the power law implicit in the coalescence model still describes our data, the coalescence parameter is observed to depend on beam energy, and the centrality of the collision. We analyze the implications of our data in the context of several coalescence models and extract information on the size of the interaction volume at freeze-out. We also determine the entropy per baryon produced in these collisions.

II. THE EXPERIMENT

The data were taken using the E814 apparatus [12–14] at the Brookhaven National Laboratory alternating gra-

dient synchrotron (AGS) facility. A multiplicity array consisting of a set of two 512 pixel silicon pad detectors located just downstream of the target measures charged particle multiplicity in the pseudorapidity range $0.8 < \eta < 3.9$. It is used for determining the centrality (related to impact parameter) of each event. A forward spectrometer accepts particles emitted in a rectangular aperture centered about the beam axis with angular dimensions of 38 mrad in the horizontal (magnetic bend) plane, and 24 mrad perpendicular to it. The spectrometer consists of two magnets, three tracking chambers, a scintillator hodoscope, and a U/Cu/Scintillator sampling calorimeter. In addition, a set of scintillators and a silicon detector are located upstream of the target for defining the beam and giving a start signal for the time-of-flight measurement.

A trigger was designed to select those events which had center-of-mass velocity charged nuclei detected in the spectrometer acceptance. It consisted of a pretrigger which determined that a beam particle had entered the apparatus and that an interaction had occurred. Valid interactions were determined by requiring that there be a minimum number of charged particles in the multiplicity detector. This threshold resulted in pretrigger cross sections of 3600 mb ($1\,\sigma_{\rm geom}$) for the Pb target, 1230 mb ($0.55\,\sigma_{\rm geom}$) for the Cu target, and 910 mb ($0.55\,\sigma_{\rm geom}$) for the Al target, where $\sigma_{\rm geom} = \pi[1.2(A_t^{1/3} + A_p^{1/3})]^2$ fm^2. In addition, in the trigger using time-of-flight information, we required the presence of a slow charged particle in a selected region of the scintillator hodoscope of the spectrometer. The spectrometer magnets were tuned such that deuterons of mid rapidity would strike the hodoscope in the center of the trigger region. Such particles will reach the scintillator wall more than 2 ns later than a particle traveling at the speed of light. The scintillator hodoscope was located 31.3 m from the target. In order to strike the trigger region, charged particles had to be deflected between 404 mm and 2828 mm in the horizontal direction at the location of the hodoscope. The trigger is satisfied when any of the scintillator slats in the trigger region registers a particle with a flight time exceeding that of a speed of light particle by more than 2 ns. The time-of-flight resolution at the trigger level was 600 ps (standard deviation σ). Off-line, the resolution (σ) was improved to be 375 ps.

In the data analysis, particles are identified by a combination of rigidity (p/q), charge (q), and time of flight measurements. We use a pattern recognition algorithm [13,15] to reconstruct tracks and determine the rigidity of each track based on its deflection in the magnetic field. The charge and time-of-flight are determined using the pulse height and timing information from the scintillator that was traversed by the particle. From these quantities the mass is then calculated. Figure 1 shows the mass distributions for identified tracks. In calculating cross sections from these data, corrections are made for inefficiencies of the detectors and of the pattern recognition algorithms. The total tracking efficiency was 69%, and with the addition of cuts on the pulse height in the scintillators was 66% for charge number $q = 1$, and 61% for $q = 2$. The detector efficiency was determined by tracking events seen in the drift chambers (which operate at nearly 100% efficiency) through the other detectors, and comparing the analysis efficiency with and without the inclusion of chosen detector planes. The targets used for the measurement had thicknesses corresponding to 2% and 4% of a ^{28}Si interaction length in Pb (2.29 and 4.52 g/cm^2), Cu (1.18 and 2.26 g/cm^2), and Al (0.65 and 1.30 g/cm^2), respectively. The total integrated beam flux was 13×10^8, 3×10^8, and 8×10^8 particles, respectively, for the Pb, Cu, and Al targets. About half of the above flux was integrated for each of the two target thicknesses. The intensity of the beam was approximately 10^5 particles per spill. Of this intensity about 40% satisfied the requirements of the beam trigger. Valid interactions therefore happened at a rate of 800 to 1600 per spill. The time-of-flight trigger reduced the number of events being recorded to magnetic tape to about 40 per spill. The data sample consisted of a total of 18849 deuterons, 632 tritons, 477 ^{3}He, and 6 ^{4}He.

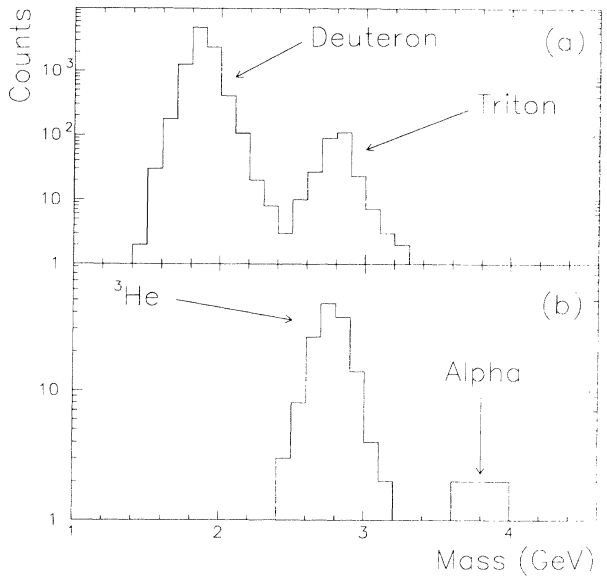

FIG. 1. Mass distributions for identified (a) charge 1 and (b) charge 2 tracks.

The detector acceptances varied with particle species, and are shown in Fig. 2. The acceptance was restricted at large p_t by the opening of the spectrometer. At high rapidities, the acceptance was restricted by a time-of-flight cut. The acceptance for the ^{4}He nuclei is different from that of the deuteron because the higher mass ^{4}He nuclei, for fixed rapidity, have a higher acceptance in p_t. They were also selected by applying a more restrictive time-of-flight cut, thereby reducing the ^{4}He acceptance at high rapidity. The largest boxes in the plot correspond to 100% acceptance, with acceptance varying linearly with the sizes of the boxes. Interactions of the produced nuclei with the material in the spectrometer and the target resulted in losses of flux of about 10%, and these losses were accounted for separately. Nontarget related background contributions to the nuclear yields were measured to be negligible.

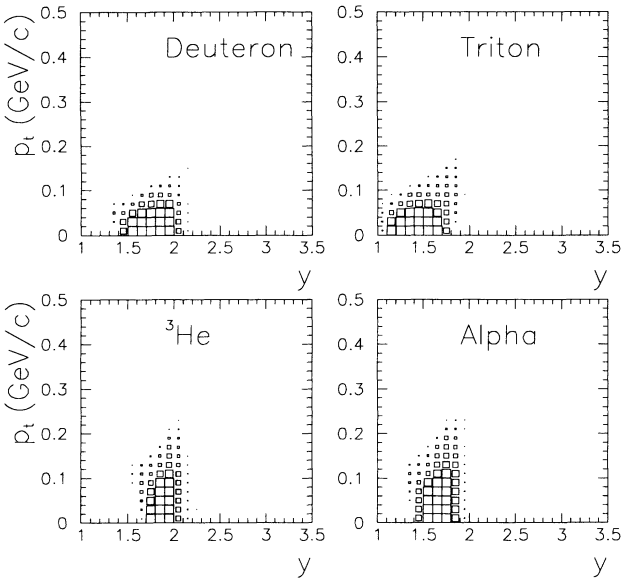

FIG. 2. The acceptance of the E814 apparatus for the detection of deuterons, tritons, ^{3}He, and ^{4}He. The largest boxes on the plot (sizes vary on a linear scale) correspond to 100% acceptance.

III. THE RESULTS

An example of the measured invariant yield, at various values of rapidity y is shown in Fig. 3 as a function of p_t for deuterons produced in 89% $\sigma_{\rm geom}$ ($\sim$ minimum bias collisions) Si+Pb interactions. Since the invariant yield varies little over the range of transverse momenta measured, the data were fit with lines of zero slope to extract the intercepts at $p_t = 0$. Our deuteron data are in good agreement with preliminary data from Experiment 802 [16] and with results from an independent measurement using the E814 spectrometer [17]. Figure 4 is a plot, as functions of rapidity, of the values of the invariant yield at $p_t = 0$ for deuterons, tritons, and ^{3}He. The upper plot shows the data for 89% $\sigma_{\rm geom}$ and the lower plot shows the data for 8% $\sigma_{\rm geom}$ (central or smallest impact parameter) events. The uncertainties shown are statistical. There is a systematic uncertainty of about 20% in the overall normalization estimated from comparisons with other E814 data. For the ^{4}He we were only able to obtain counts in the 55% $\sigma_{\rm geom}$ analysis. The invariant yields were measured to be $(1.6 \pm 1.2) \times 10^{-4}$ and $(0.5 \pm 0.4) \times 10^{-4}$ GeV^{-2}c^2 at rapidities of $1.4 \rightarrow 1.6$, and $1.8 \rightarrow 2.0$, respectively.

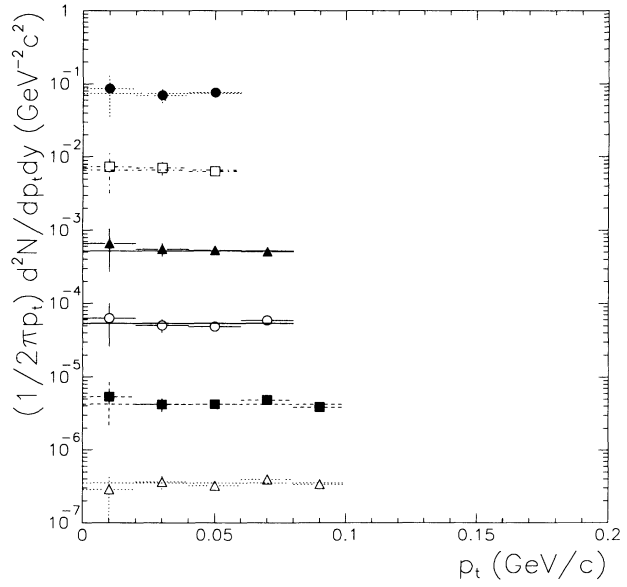

FIG. 3. The invariant yield of deuterons plotted as a function of p_t, in rapidity intervals of 0.1 unit, for 89% $\sigma_{\rm geom}$ Si+Pb collisions. The top curve corresponds to $1.4 < y < 1.5$ and the bottom curve to $1.9 < y < 2.0$. The data have been divided by successive factors of 10 for visual clarity. Uncertainties are statistical only.

IV. DISCUSSION

It is unlikely that the nuclei we measure at central rapidity are fragments of the target or projectile. In order to be decelerated down to center-of-mass velocities from the projectile velocity, or accelerated up from the target velocity, the nuclei would have to endure collisions that would undoubtedly dissociate them into their constituent nucleons. Consequently, these nuclei must be formed in the region of highly excited nuclear matter.

In the empirical coalescence model [10,11,18], the invariant cross section for the production of a cluster with mass number A is related to the probability that A nucleons are emitted with relative momenta less than the coalescence momentum $\tilde{p}_0$ (i.e., spatial proximity is ignored). This furnishes a relation between the cross sec-

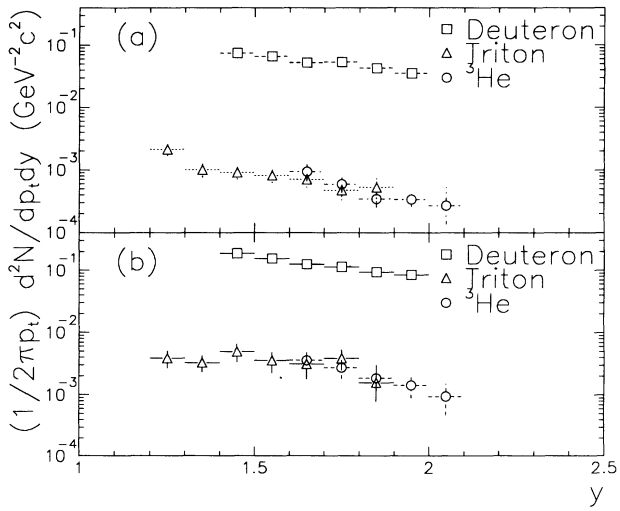

FIG. 4. The invariant yields of deuterons, tritons, and ^{3}He at $p_t = 0$ plotted as a function of rapidity for Si+Pb collisions. Multiplicity cuts correspond to (a) 89% and (b) 8% , respectively, of the geometrical cross section. The uncertainties shown are statistical only.

tion for emitting a nuclear cluster with a momentum p_A and that for emitting a nucleon with momentum p_p . This relation can be expressed as

$$E_A \frac{d^3N_A}{dp_A^3} = B_A \left(E_p \frac{d^3N_p}{dp_p^3} \right)^A , \quad (1)$$

where $p_A = Ap_p$. The dimensioned scale factor, B_A, is given by [19]

$$B_A = A \frac{2s_A + 1}{2^A} R_{np}^N \frac{1}{N!Z!} \left(\frac{4\pi}{3m} \tilde{p}_0^3 \right)^{A-1} , \quad (2)$$

where s_A is the spin of the cluster, m is the mass of the proton, R_{np} is the ratio of the total number of neutrons to protons in the target and projectile, and N and Z are the neutron and proton number of the composite particle. This relation assumes that the shapes of the proton and neutron spectra are identical. The coalescence momentum characterizes the maximum amount of relative momentum that the nucleons can have and still coalesce into a single nucleus. B_A should be constant for a given nuclear species since it depends only on parameters of the cluster (except for a slight target-projectile dependence through R_{np}). In fact, many experiments at the Bevalac [9] found that B_A was fairly independent of beam energy, the momentum of the cluster, or angle of emission. This is shown in Fig. 5 where the values of B_A measured for Ne+Pb collisions for deuterons, tritons, and ^{3}He [20] are plotted as a function of the total kinetic energy per nucleon of the beam. Some differences in B_A were seen for different colliding partners.

Our data set did not include an adequate sample of protons in the kinematic regions of interest and measured under identical trigger conditions. However, the ARC model (A Relativistic Cascade, version 1.15) [21–23] provides a good description of the proton data measured by our experiment at central rapidities and low p_t in central collisions [14,24–26]. Descriptions of similar quality (agreement at the level of 10%) are obtained for the data from experiment E802 [16] at large p_t over a wide range of rapidities for minimum bias and central collisions [23]. We therefore used ARC as a source of proton spectra. The ARC simulated data set consisted of the results of 5 $\times 10^3$ Si + Pb collisions and 10^4 collisions of Si with Cu and Al. A charged particle multiplicity was calculated for each ARC event by determining the number of charged particles traveling into the angular acceptance of the silicon multiplicity detectors. The ARC charged particle multiplicity spectrum agrees well [14] with that measured by E814. The ARC events are sorted into centrality bins in the same manner as the data, and were used to calculate B_A. The systematic error in B_A owing to the use of ARC spectra instead of data is estimated to be about 15% from comparisons to proton data. As discussed above, the coalescence parameter B_A should not depend on the particular reaction and kinematics where the cluster is produced. In particular, B_A should be independent of p_t and y of the cluster. Figure 6 shows the y dependence of B_A for d, t, and ^{3}He production in 89% σ_{geom} Si+Pb collisions. Within the fairly large statistical errors, B_A is indeed approximately independent of y.

However, a striking departure from the coalescence model is found by examining the centrality dependence of B_A. Figure 7 shows B_A for several exclusive centrality bins. The exclusive centrality bins represent small slices of the charged particle multiplicity spectrum, and thus are an attempt to approximate nonoverlapping ranges of impact parameter. The extremities of each bin have been defined in terms of a variable C_i which can be evaluated

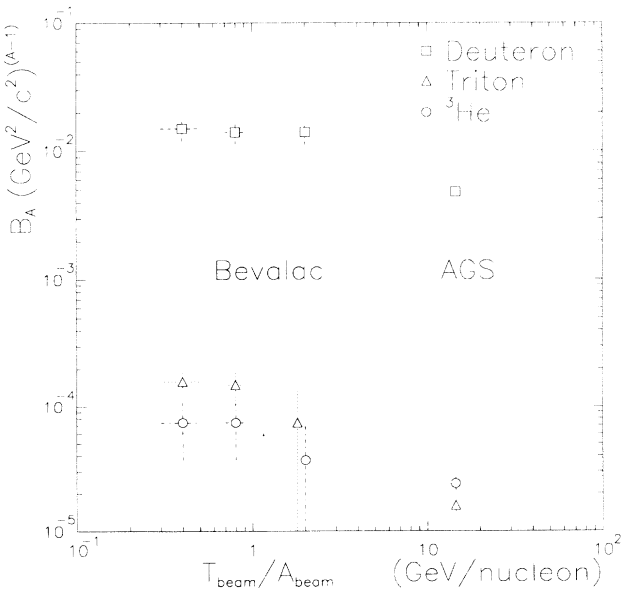

FIG. 5. Coalescence scaling coefficient, B_A, plotted as a function of incident beam kinetic energy per nucleon. The points for the lowest three energies are from Ne+Pb interactions [20]. The highest energy data points are from this work. All data were measured in minimum-bias collisions.

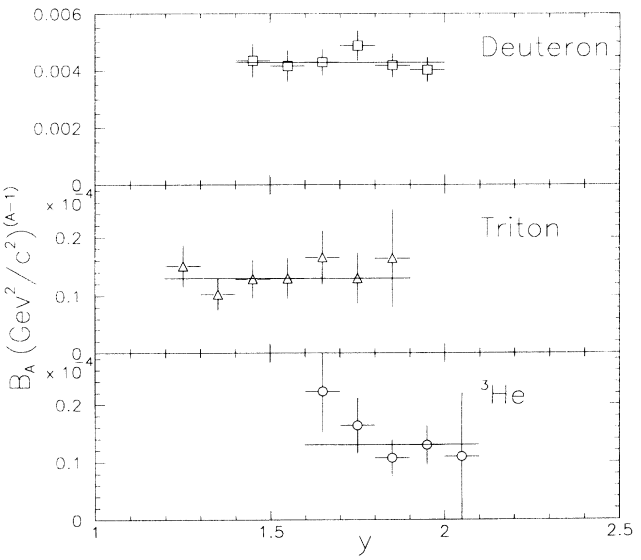

FIG. 6. The coalescence scaling coefficient, B_A, plotted as functions of rapidity for d, t, and ^{3}He in 89% σ_{geom} Si+Pb collisions.

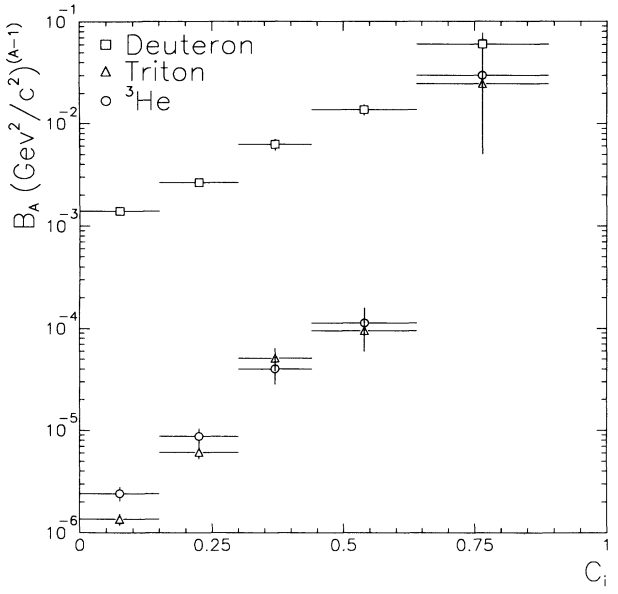

FIG. 7. The coalescence scaling coefficient B_A plotted as a function of centrality for deuterons, tritons, and ^{3}He from Si+Pb collisions. The points plotted denote average values of the centrality range represented by the horizontal error bar. Uncertainties shown are statistical only.

using the charged particle multiplicity distributions measured by the Si detector as

$$C_i = \frac{\int_{N_{C_i}}^{\infty} \frac{d\sigma}{dN_c} dN_c}{\int_0^{\infty} \frac{d\sigma}{dN_c} dN_c}, \tag{3}$$

where N_{C_i} is the charged particle multiplicity corresponding to the lower limit of one of the above integrals. All events within a selected range of multiplicity ($N_{C_i} \rightarrow N_{C_j}$) would then be used to calculate B_A for a particular centrality bin. Low values of C_i correspond to the most central events.

From Fig. 7 we see that there is a very strong dependence of B_A on the centrality of the collision. As collisions progress from the most central to the most peripheral, the value of B_A increases for the Si+Pb system by about a factor of 45 for deuterons and 10^4 for mass 3 nuclei. This is a clear departure from what is expected in the basic coalescence model. Our results imply that the coalescence of nucleons into clusters is profoundly influenced by the dynamics of the collision, and not just the intrinsic properties of the cluster. Earlier measurements at the Bevalac did imply that a single scale factor did not describe both minimum bias and central data [27]. Also, the energy and multiplicity dependence of fragment production was studied in the context of entropy production [28]. Our results, however, constitute the first investigation of the variation of the coalescence scale factor as a function of centrality. The study of coalescence as functions of centrality obviates the need to consider problems associated with impact parameter averaging [10], in particular, the effects of momentum correlations arising as a result of hydrodynamic flow.

An additional discrepancy with the simple coalescence model is the observation that B_A changes significantly as the beam kinetic energy is raised from Bevalac values of 1–2A GeV to AGS values of 10-15A GeV. Our data points in Fig. 5 show that B_A drops by about a factor of 3 at AGS energies relative to the Bevalac value.

A possible explanation for our results may require a consideration of the spatial correlations of the coalescing nucleons. The simple coalescence model requires only that the nucleons be close to each other in momentum space, but no account is taken of the nucleons' spatial proximity to each other. In collisions at Bevalac energies, the number of produced particles is small, and source sizes are on the order of the size of the incident nucleus, i.e., 3–4 fm. This size is comparable to that of the coalesced nuclei. Thus, spatial proximity is not a consideration. However, for the higher energy collisions at the AGS, it is reasonable to expect a significant amount of expansion of the system before the densities are low enough to allow coalesced nuclei to survive. The expansion is also indicated by our pion correlation data [5]. The beam energy dependence of the coalescence scale factor may be signaling the entrance into a regime where spatial separations of the coalescing nucleons must be taken into account.

An alternative description of the data may be obtained using the thermodynamic model [19]. It predicts a power-law dependence of nuclear yields similar to the simple coalescence model. The centrality dependence of B_A is related to the freeze-out volume of the collision region. The model is nonrelativistic, and assumes that thermal and chemical equilibrium are achieved, and that the nuclei are produced uniformly over the collision volume. There is some experimental support for the equilibrium assumption based on this and other measurements using the E814 apparatus [5,29]. We do not elaborate on this model further because its predictions are qualitatively similar to the discussion that follows.

A model based on a density matrix formulation of the many body problem has been developed by Sato and Yazaki [30], and improves on the simple coalescence and thermodynamic models. It circumvents the need to make assumptions about thermal and chemical equilibrium by relying on a dynamical picture of coalescence. The model assumes that in the collision, a highly excited region is formed which decays by emitting various particles. The momentum distribution of nucleons within this region, as well as the emitted particles, are approximately described by density matrices. The model assumes explicit forms for the wave functions and the spatial distribution of nucleons in the excited region. By choosing Gaussian distributions for these functions, the model can be cast in the same form as the empirical coalescence model and one can relate the coalescence momentum $\tilde{p}_0$ to the size parameter of the excited region ν as

$$\frac{1}{N!Z!}\left(\frac{4\pi}{3}\tilde{p}_0^3\right)^{A-1} = A^{\frac{1}{2}}\left(4\pi\frac{\nu_A\nu}{\nu_A+\nu}\right)^{\frac{3}{2}(A-1)}, \tag{4}$$

where ν_A are the parameters of the Gaussian wave functions and the size parameter ν is related to the root mean squared (rms) radius of the excited region as

$$R_{\rm rms} = \sqrt{\frac{3}{2\nu}}. \quad (5)$$

The values used for the wave function parameters for the mass 2 and mass 3 systems are $\nu_2 = 0.20$ fm^{-2} and $\nu_3 = 0.36$ fm^{-2}, respectively [31].

Applying this method to our data yields the results shown in Table I for several targets and for similar inclusive centrality bins. We plot in Fig. 8, the radius $R_{\rm rms}$ so obtained, for exclusive centrality bins in Si+Pb interactions.

The most central collisions exhibit much larger radii than the more peripheral ones. The radii corresponding to the most peripheral collisions are smaller than the impact parameter averaged radii. In the context of this model one would conclude that there is expansion of the collision volume before freeze-out since the extracted radii are significantly larger than the projectile, for central collisions. For example, the rms charge radii of the Si and Pb nuclei are measured to be 3.04 fm and 5.42 fm, respectively [32].

Figure 8 also shows some dependence of the radii on the cluster mass, which in this model could be interpreted as different nuclei freezing out at different times. The radius parameters calculated for deuterons are consistently higher than those calculated for both mass 3 nuclei. This would imply that the mass 3 nuclei freeze out at earlier times. Such a scenario makes intuitive sense when one considers the fact that the mass 3 nuclei have much higher binding energies than deuterons. The binding energy of a deuteron is 2.2 MeV, which makes it barely bound, and it is therefore not likely to survive many collisions before being dissociated.

There are two weaknesses in the model of Sato and Yazaki [30]. First, this model is not relativistic. Second, the model makes a Gaussian approximation for the spatial distribution of nucleons within the source. This might explain why the radii shown in Fig. 8 differ from other estimates of source size. The source size determined from the deuteron yield in central collisions ($R_{\rm rms}$ = 7.1 fm) can be compared to the result obtained from the two pion HBT correlation [5]. There, the data are found to be consistent with a pion source distribution as predicted by the relativistic Quantum Molecular Dynamics (RQMD version 1.07), model [33] with $R_{\rm rms}$ = 8.3 fm. The radius parameter extracted from coalescence data does show many intuitively satisfying trends. However, in light of the shortcomings of the model, caution is warranted in the interpretation of the actual values.

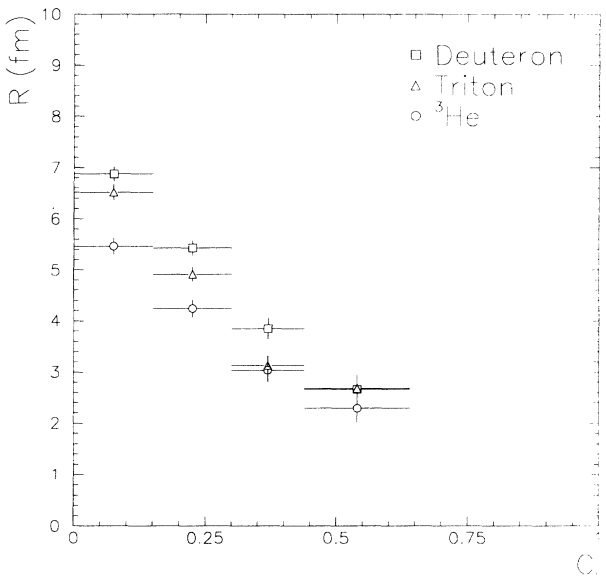

FIG. 8. Radius parameter deduced using the model of Sato and Yazaki [30]. The results are plotted as a function of centrality for deuterons, tritons, and ^{3}He created in Si+Pb collisions. The values plotted are averages values of the rms radius for the centrality range represented by the horizontal error bar.

TABLE I. Coalescence model radius parameter $R_{\rm rms}$ obtained using the model of Sato and Yazaki [29] for deuterons, tritons, and ^{3}He, for various centralities and targets. The 89% $\sigma_{\rm geom}$ events represent mimimum bias collisions, and the 8% $\sigma_{\rm geom}$ events represent central collisions. The 55% $\sigma_{\rm geom}$ events were chosen to compare all three targets.

Target and centrality	Nucleus		
	^{2}H	^{3}H	^{3}He
89% $\sigma_{\rm geom}$			
Si+Pb	4.5 ± 0.1	4.2 ± 0.1	3.9 ± 0.1
55% $\sigma_{\rm geom}$			
Si+Pb	5.2 ± 0.1	5.0 ± 0.1	4.4 ± 0.1
Si+Cu	3.6 ± 0.1	2.7 ± 0.1	2.5 ± 0.1
Si+Al	2.9 ± 0.1	2.3 ± 0.1	2.5 ± 0.2
8% $\sigma_{\rm geom}$			
Si+Pb	7.1 ± 0.2	6.5 ± 0.2	5.1 ± 0.2

Cascade calculations provide a more realistic description of the reaction than the thermodynamic or density matrix models discussed above. The advantage of using a cascade calculation is that many of the problems of the previously discussed models, such as relativistic considerations, hydrodynamic flow, and differences in the kinematic distributions of protons and neutrons, are taken into account in the dynamics of the cascade. Assumptions about the equilibrium properties and shapes of the system are not necessary. Some assumptions and approximations are inevitably present, but the success that ARC and RQMD have had in reproducing baryon and meson distributions lends credibility to the calculations. These models have to be extended to allow calculation of the abundances of composite particles. Dover and Baltz [34] have formulated such an extension. In their model, for nucleons to coalesce they must be close to each other in both position and momentum after they have stopped interacting. In some sense this is analogous to the basic coalescence model previously discussed. The major differences are that cascade based coalescence is considered on a microscopic level (i.e., individual nucleons from the cascade are coalesced), and spatial separations are taken into account.

First calculations have been performed within the ARC framework for Si + Au and Au + Au collisions at AGS en-

ergies [34]. The results compare favorably with measurements of deuteron dN/dy for $y < 1.4$ in central Si + Au collisions from E802, and preliminary data on deuterons, tritons, ^{3}He, and ^{4}He at target rapidities in minimum bias Au + Au collisions from E886 [34]. A comparison of the ARC coalescence results with our data is presented in Fig. 9. The calculation was performed for central (highest 7% of the total cross section) Si + Au collisions. The agreement of the calculation with the data is reasonable. The deuteron cross section is overpredicted by somewhat less than a factor of 2. One should note that no fits are performed to the shapes of the spectra. The only adjustable parameters are the maximum spatial and momentum separations of the nucleons in order for them to coalesce. Their values only affect the normalization, and are constrained by data from E802 and E886, as well as the data presented here. The ARC model can now be used to estimate the production cross sections of multistrange hypernuclear objects, and strangelets [34].

Coalescence calculations using the cascade code RQMD provide an excellent description of the yields of light nuclei [35] measured by the E814, E802, and E878 experiments. The results of this calculation have also been shown in Fig. 9. In addition, the RQMD model has been used to extract the dimensions of the collision volume at freeze-out. The collision volume is determined from the location where the deuterons are created and has a transverse radius of $R_T = 5.3$ fm, and a longitudinal radius of $R_L = 4.3$ fm, for central (10% $\sigma_{\rm geom}$) Si+Pb collisions. The corresponding rms radius for the deutron source is 6.8 fm, very close to the 7.1 fm shown in Table I. The deuterons chosen for this calculation were created within ± 0.6 units of central rapidity.

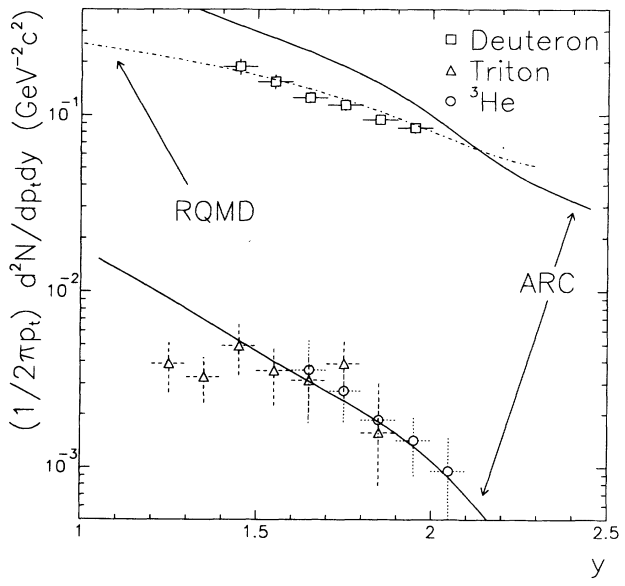

FIG. 9. First results from an ARC coalescence calculation (solid lines) [34] and from an RQMD coalescence calculation (dashed line) [35]. The points are the measured invariant yields at $p_t = 0$ for 8% $\sigma_{\rm geom}$ Si+Pb collisions. The ARC curves have been calculated for 7% $\sigma_{\rm geom}$ in Si+Au collisions for deuterons and mass 3 particles. The RQMD curves are shown for deuterons produced in 8% $\sigma_{\rm geom}$ Si+Pb collisions.

We can use our data to calculate the baryon density of the collision volume at freeze-out. If we assume that the $N_n = 138$ baryons contained in the region of overlap of the Si and Pb nuclei, at zero impact parameter, are contained in a volume of uniform density of radius $\sqrt{\frac{5}{3}} \times 7.1$ fm (to convert from an rms radius of 7.1 fm to a total radius) we obtain a baryon density of 138/3226 $= 0.043$ /fm^3. This is approximately one quarter of the baryon density of the projectile or target nuclei in their rest frames. Using other data measured by our experiment, we have determined the pion density at freeze-out to be ~ 0.061 /fm^3 [29]. The entropy per baryon (including the contribution of pions) is given by [8,36]

$$\frac{S}{A} = 3.945 - \ln(d/p) + 4.1\frac{N_\pi}{N_n} \sim 12.8\ , \qquad (6)$$

where d/p is the ratio of deuteron yields to proton yields. For this calculation, the ratio is assumed to be the ratio 0.012 of the respective invariant cross sections measured at $p_t = 0$. The number of secondary pions, N_π, is 150. The numbers for N_n and N_π have been obtained from data and from RQMD model calculations. The entropy per baryon, 12.8, exceeds the value of 6 measured at Bevalac energies [10], and is consistent with the entropy expected of a mixed quark-hadron phase [37].

V. SUMMARY

The data presented here are some of the first measurements of mass 2, 3, and 4 nuclei produced at midrapidities in Si-nucleus collisions at 14.6 GeV/nucleon. The power-law production implicit in the empirical coalescence model was found to adequately describe our data; however, the interpretation of the model was found to be unsatisfactory. A strong dependence of the scale factor B_A on the centrality of the collision as well as beam energy has been observed, and implies that the coalescence momentum is not a universal parameter which depends only on the type of cluster produced. This behavior signals the entrance into a regime where the simple picture of coalescence in momentum space, with no regard for physical proximity of the nucleons, is no longer adequate. A more reasonable interpretation is supplied by the coalescence model of Sato and Yazaki, which also embodies power-law production, but relates the scale factor to the volume of the emitting system. This model furnishes an interpretation of the dependence of the scale factor on centrality and beam energy. By taking advantage of the dependence of this model on the volume, we have determined the size of the emitting source from relative yield measurements of the light nuclei studied. The radii so determined indicate that the system undergoes a significant amount of expansion. The source sizes associated with central collisions are larger than those of the target and projectile nuclei. We determine the entropy per baryon in central collisions to be ~ 12.8, which is consistent with the creation of a mixed quark-hadron phase.

Our measurements indicate that the nucleus-nucleus collision volume may remain coupled for much longer than was previously assumed, a result which is in agreement with two pion HBT studies using the E814 apparatus [5]. There is, however, some caution warranted in the interpretation of the radius calculated from coalescence models as the actual size of the system. Although the radius shows the trends expected with centrality and colliding target and projectile nuclei, an independent confirmation, or calibration, of this technique is needed.

Some very promising means of understanding the formation of light nuclei, and possibly providing such a calibration of the source size calculation, are the coalescence models based on ARC and RQMD. These models have had reasonable success reproducing the results from several experiments, as well as a subset of the data presented here. The work on providing detailed descriptions of cluster production using cascade models is still in its infancy. We look forward to further results from the ARC and RQMD coalescence calculations, and the possible insights they can give on source size and freeze-out phenomena.

ACKNOWLEDGMENTS

We thank the AGS staff and Dr. H. Brown for providing us with beam, and J. Sondericker III and R. Hutter for technical support. We also thank S. Voloshin and J. Nagle for a careful reading of this manuscript. This work was supported in part by the U.S. DOE, the NSF, NSERC, Canada, and CNPq, Brazil.

[1] E814 Collaboration, J. Barrette *et al.*, Phys. Rev. Lett. **70**, 2996 (1993); and articles in *Quark Matter '91* [Nucl. Phys. **A544** (1992)].
[2] W. Zajc, in *Particle Production in Highly Excited Hadronic Matter*, edited by H. Gutbrod and J. Rafelski, NATO ASI Series B: Physics (Plenum, New York, 1993), Vol. 303, p. 435.
[3] E802 Collaboration, T. Abbott *et al.*, Phys. Rev. Lett. **69**, 1030 (1992).
[4] E814 Collaboration, N. Xu, in *Heavy Ion Physics at the AGS*, edited by G. S. F. Stephans, S. G. Steadman, and W. L. Kehoe, MITLNS-2158 (Cambridge, MA, 1993), p. 362.
[5] E814 Collaboration, N. Xu *et al.*, Nucl. Phys. **A566**, 585c (1994); E814 Collaboration, J. Stachel *et al.*, *ibid.*, **A566**, 183c (1994).
[6] J. Schaffner *et al.*, Phys. Rev. Lett. **71**, 1328 (1993); Ann. Phys (N.Y.) (to be published).
[7] E. Farhi and R.L. Jaffe, Phys. Rev. D **30**, 2379 (1984); **32**, 2452 (1985).
[8] P. Siemens and J. Kapusta, Phys. Rev. Lett. **43**, 1486 (1979).
[9] S. Nagamiya *et al.*, Annu. Rev. Nucl. Part. Sci. **34**, 155 (1984).
[10] L.P. Csernai and J.I. Kapusta, Phys. Rep. **131**, 223 (1986).
[11] H. H. Gutbrod *et al.*, Phys. Rev. Lett. **37**, 667 (1976); M.-C. Lemaire *et al.*, Phys. Lett. **85B**, 38 (1979); B.V. Jacak *et al.*, Phys. Rev. C **35**, 1751 (1987).
[12] E814 Collaboration, J. Barrette *et al.*, Phys. Rev. Lett. **64**, 1219 (1990).
[13] E814 Collaboration, J. Barrette *et al.*, Phys. Rev. C **45**, 819 (1992).
[14] J. Germani, Ph.D. thesis, Yale University, 1993.
[15] J.T. Mitchell, Ph. D. thesis, Yale University, 1992.
[16] C. Parsons, Ph. D. thesis, MIT, 1992.
[17] E814 Collaboration, J. Dee and B. Hong *et al.* (unpublished).
[18] A. Schwarzschild and Č. Zupančič, Phys. Rev. **129**, 854 (1963).
[19] S. Das Gupta and A.Z. Mejkian, Phys. Rep. **72**, 131 (1981).
[20] S. Nagamiya *et al.*, Phys. Rev. C **24**, 971 (1981).
[21] Y. Pang, T.J. Schlagel, and S.H. Kahana, Phys. Rev. Lett. **68**, 2743 (1992).
[22] T.J. Schlagel, S.H. Kahana, and Y. Pang, Phys. Rev. Lett. **69**, 3290 (1992).
[23] S. Kahana in *Heavy Ion Physics at the AGS* [4], p. 263.
[24] E814 Collaboration, J. Dee *et al.*, in *Heavy Ion Physics at the AGS* [4], p. 47.
[25] E814 Collaboration, Z. J. Barrette *et al.*, Phys. C **59**, 211 (1993).
[26] B.S. Kumar and J.V. Germani, notes to the E814 collaboration, Yale 40609-1143 (unpublished).
[27] S. Hayashi *et al.*, Phys. Rev. C **38**, 1229 (1988).
[28] K.G.R. Doss *et al.*, Phys. Rev. C **32**, 116 (1985); **37**, 163 (1988).
[29] E814 Collaboration, P. Braun-Munzinger, in *Hot and Dense Nuclear Matter*, Proc. NATO Advanced Study Institute, Bodrum, Turkey, Oct. 1993 (Plenum, New York, in press).
[30] H. Sato and K. Yazaki, Phys. Lett. **98B**, 153 (1981).
[31] J.C. Bergstrom, Nucl. Phys. **A327**, 458 (1979).
[32] R. Hofstadter, Rev. Mod. Phys. **28**, 214 (1956).
[33] H. Sorge, H. Stöcker, and W. Greiner, Ann. Phys. (N.Y.) **192**, 266 (1989).
[34] C.B. Dover *et al.*, Brookhaven Internal Report No. BNL-48594; in *Heavy Ion Physics at the AGS* [4]; p. 213; A.J. Baltz, C.B. Dover, S.H. Kahana, Y. Pang, T.J. Schlagel, and E. Schnedermann, Phys. Lett. B **325**, 7 (1994).
[35] J. Nagle *et al.*, Yale-40609-1139 (unpublished).
[36] S.Z. Belenkij and L.D. Landau, Nuovo Cimento, Supplement **3**, 15 (1956), reprinted as article 88 in *Collected papers of L.D. Landau*, edited by D.Ter Haar (Gordon and Breach, New York, 1965).
[37] H. von Gersdoff *et al.*, Phys. Rev C **39**, 1385 (1989).